Biophysical Journal Volume 67 October 1994 1706–1712

pH-Induced Structural Changes in Bacteriorhodopsin Studied by Fourier Transform Infrared Spectroscopy

Sándor Száraz,* Dieter Oesterhelt,‡ and Pál Ormos*

*Institute of Biophysics, Biological Research Centre of the Hungarian Academy of Sciences, H-6701 Szeged, Hungary, and ‡Max-Planck-Institute for Biochemistry, D-82152 Martinsried, Germany

ABSTRACT Previous C^{13}-NMR studies showed that two of the four internal aspartic acid residues (Asp-96 and Asp-115) of bacteriorhodopsin (bR) are protonated up to pH = 10, but no accurate pK_a of these residues has been determined. In this work, infrared spectroscopy with the attenuated total reflection technique was used to characterize pH-dependent structural changes of ground-state, dark-adapted wild-type bacteriorhodopsin and its mutant (D96N) with aspartic acid-96 replaced by asparagine. Data indicated deprotonation of Asp-96 at high pH ($pK_a = 11.4 \pm 0.1$), but no Asp-115 titration was observed. The analysis of the whole spectral region characteristic to complex conformational changes in the protein showed a more complicated titration with an additional pK_a value ($pK_{a1} = 9.3 \pm 0.3$ and $pK_{a2} = 11.5 \pm 0.2$). Comparison of results obtained for bR and the D96N mutant of bR shows that the $pK_a \approx 11.5$ characterizes not a direct titration of Asp-96 but a protein conformational change that makes Asp-96 accessible to the external medium.

INTRODUCTION

Bacteriorhodopsin (bR) is a pigment-protein complex with a retinal chromophore. It is located in the purple membrane (PM) of *Halobacterium halobium* and functions as a light-driven proton pump (for review, see Stoeckenius and Bogomolni, 1982; Oesterhelt and Tittor, 1989; Mathies et al., 1991; Ebrey, 1993; Lanyi, 1993). The retinal chromophore is bound to Lys-216 via a protonated Schiff-base. The absorption of light initiates the photocycle of bR, in which the molecule passes several spectrally distinct metastable states before it returns to the initial state. The simplest photocycle scheme that can explain most of the experimental findings contains five intermediates arranged sequentially: bR-K-L-M-N-O-bR (Lozier et al., 1975). During this cycle, a proton is transported from the cell to the extracellular medium in several distinct steps that are synchronized to those in the photocycle (Keszthelyi and Ormos, 1989).

Experimental data obtained by different measuring techniques have shown that structural changes of both the retinylidene Schiff-base chromophore (for overview, see Mathies et al., 1991) and the protein (Koch et al., 1991; Dencher et al., 1991; Ormos et al., 1991; Subramaniam et al., 1993) occur during the photocycle. The availability of site-specific mutants of bR allowed the assignment of the amino acid residues that take part in the proton transport process (Rothschild and Marrero, 1982; Bagley et al., 1982; Dollinger et al., 1986; Braiman et al., 1988; Gerwert et al., 1989, 1990, 1992; Ormos et al., 1991, 1992). These data and investigation of alterations in transport properties of these mutants (Mogi et al., 1988; Holz et al., 1989, Butt et al., 1989, Tittor et al., 1989) showed that aspartic acid residues in positions 85, 96, and 212 are crucial in the pumping process. From FTIR difference spectroscopy, it was concluded that Asp-85 and Asp-212 are deprotonated, that Asp-96 is protonated in the initial state, and that these residues transiently change their protonation state during the photocycle. Based mostly on these findings and the structural model of bacteriorhodopsin (Henderson et al., 1990), a widely accepted model for the mechanism of the bR proton pump has been created (Fodor et al., 1988; Mathies et al., 1991; Oesterhelt et al., 1992; Ebrey et al., 1993). It involves proton transfers between the retinal Schiff-base and several aspartate residues. The following steps are regarded as crucial: first, the Schiff-base proton is transferred to Asp-85, which then causes a proton release to the external medium from an as yet undetermined group; this is followed by the transfer of a proton from Asp-96 to reprotonate the Schiff-base; then Asp-96 is subsequently reprotonated from the cytoplasmic side of the membrane; finally, Asp-85 deprotonates.

This mechanism implies that Asp-96 is protonated in the initial state (Lanyi et al., 1993, Mathies et al., 1991). Solid state ^{13}C NMR measurements showed that two aspartic acid residues (96 and 115) are protonated up to pH = 10 (Metz et al., 1992) but no pK_a for these groups were specified. Recently, the effects of solvation and charge-charge interactions on the pK_a of the ionizable groups in bacteriorhodopsin have been studied using a macroscopic dielectric model in computational theoretical studies. Calculations showed that the predicted pK_a values are highly dependent on the orientation of the side chain of Arg-82 (Bashford and Gerwert, 1992), whose placement is ambiguous in the structure derived from electron density maps (Henderson et al., 1990). Best agreement with experimental data was achieved if this side chain points toward the Schiff-base. In this case, the calculations gave $pK_a = 11.6 \pm 1.2$ for Asp-96 and $pK_a = 15.4 \pm 8.6$ for Asp-115.

In the present study, we have applied difference infrared spectroscopy combined with the attenuated total reflection

Received for publication 26 April 1994 and in final form 25 July 1994.

Address reprint requests to Dr. Pal Ormos, Institute of Biophysics, Biological Research Center of the Hungarian Academy of Sciences, Temesvari krt. 62/H-6701 Szeged, Hungary. Tel.: 36-62-432232; Fax: 36-62-433133.

0006-3495/94/10/1706/07 $2.00

(ATR) technique to obtain further experimental information on pH-induced structural changes of the bR initial state. This technique allows the easy and accurate control of pH in the bathing solution of the purple membranes (Marrero and Rothschild, 1987). These studies permitted us to determine accurate pK_a values for deprotonation of Asp-96 and pH-induced changes of the protein structure.

MATERIALS AND METHODS

Instrumentation

Infrared spectra were recorded on a PU9800 Fourier-transform infrared spectrometer (Philips, Cambridge, UK) equipped with a DTGS detector and an external horizontal attenuated total reflection (ATR) accessory (Spectratech Inc., Stamford, CT). This cell includes a 45° trapezoidal germanium plate and is designed for liquid samples.

Sample preparation

Purple membranes (PM) were isolated from *H. halobium* strain ET1001 according to Oesterhelt and Stoeckenius (1974). The D96N mutant was prepared from a derived mutant strain of *H. halobium* using the procedure described in Soppa et al. (1989a, b).

For the measurements, purple membranes were suspended in tridistilled water yielding 0.6 mM bacteriorhodopsin concentration. 400 μl of this suspension was dried on the surface of the germanium plate of the ATR cell (see Fig. 1) in vacuum. Then the cell was filled with 2 ml of 1 M NaCl solution (pH = 7). Hydration and stability of the PM film were checked by subtracting consecutively measured spectra. The sample stabilized in about a day. The pH of the bathing solution was changed in the range of pH ≈ 7–12.5 by adding appropriate amounts of concentrated NaOH or HCl and was continuously monitored using a micro-combination pH-electrode (model PHR-146, Lazar Research Laboratories, Inc., Los Angeles, CA). Single beam infrared spectra (1000 scans, 2-cm^{-1} resolution) were taken at very low ambient light intensity where the sample could be considered dark-adapted. It was necessary to work in the dark: depending on the pH, the lifetime of M changes; it becomes very long, especially at high pH, and the sample practically bleaches. Controlled light adaptation at high pH, therefore, is not possible. Fortunately, as we will see later, working with dark-adapted bR did not cause problems in our conclusions.

Data processing

All spectral manipulations were carried out by home-written programs using Matlab for Windows software (MathWorks, Natick, MA). First, single-beam spectra were normalized in the 1800–2000 cm^{-1} region to compensate small drifts of spectra in time. Difference absorption spectra for a given pH = X was calculated using the formula

$$\Delta A(\bar{\nu})_{pH=X} = -\log_{10} I(\bar{\nu})_{pH=X}/I(\bar{\nu})_{pH=7}), \quad (1)$$

where $I(\bar{\nu}_{pH=X}$ is a single-beam spectrum taken at pH = X and $\bar{\nu}$ is wavenumber. To analyze quantitatively the pH dependence of the spectra, singular value decomposition (SVD) of the data set (difference spectra at all pHs) was applied. For mathematical definition of SVD and its application for data analysis see, e.g., Henry and Hofrichter (1992); here we describe only its use for our special case. In general, our procedures are related to those applied by Turner et al. (1993), who investigated pH titration by visible spectroscopy. SVD is a very convenient tool because it gives a set of orthonormal basis spectra ordered by decreasing weight and also their associated amplitude as a function of pH. If the measured spectra are organized as columns of a matrix A, SVD decomposes A as a product of three matrices:

$$A = U \cdot S \cdot V^T, \quad (2)$$

where columns of U contain the basis spectra, S is diagonal and contains the corresponding weights, whereas the columns of V give the pH dependence of the basis spectra (both U and V are column-orthonormal). The most important property of SVD is that each subset of the first n components in U provides the best basis for an n component approximation of the data matrix in a least-squares sense. This way it is usually possible to select a reduced number of basis spectra that represent the data matrix within the experimental precision. A very important advantage of SVD is that it helps to find the number of independent spectral components without any assumption about the shape.

The pK_a for a specific process reflected by a given basis spectrum was determined by least-squares fitting of the corresponding column of V by a two parameter function derived from the Henderson-Hasselbalch equation:

$$V_i = \sum_{i=1}^{n} C_i/(1 + 10^{(pK_i - pH)}, \quad (3)$$

where the varied parameters were: C_i, proportional to the concentration of groups showing spectral changes in the wavenumber region selected for SVD; pK_i, the midpoint of titration. (Curve fitting was performed using the Nelder-Mead simplex algorithm built into Matlab.)

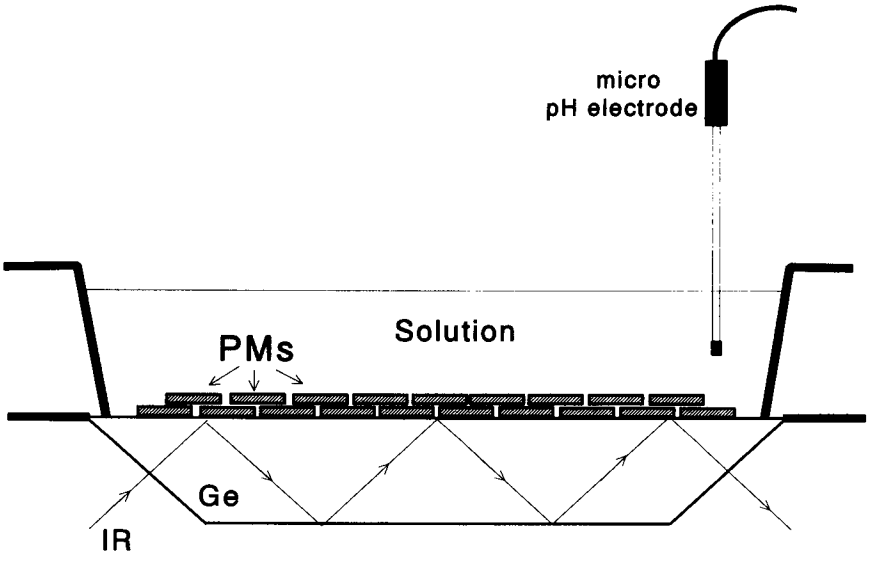

FIGURE 1 Scheme of the sample compartment.

In each case, at least three independent experiments were performed. The reported pK_a values and their errors originated from the mean and SD calculated from the results of the individual fits, respectively.

RESULTS

Fig. 2, *A* and *B* show a sequence of ATR difference spectra of wild-type bacteriorhodopsin and the D96N mutant calculated using Eq. 1. In the wavenumber region shown (1400–1800 cm^{-1}), these spectra reflect structural changes of the protein backbone, the retinal chromophore, and also protein side chains. (Unfortunately, in control experiments, where only the bathing solution (1 M NaCl) was titrated, a huge and broad peak appeared around 1400 cm^{-1}, probably because of the increasing amount of nondissociated NaOH at higher pH. Because of this problem, the spectral region below 1400 cm^{-1} has been omitted.) The difference spectra are dominated by two bands located at 1661 cm^{-1} (amide-I band, C=O vibration) and 1542 cm^{-1} (amide-II band, NH-bending vibration), respectively, which are characteristic of vibrations of the protein backbone and are the major feature of all protein spectra. At first glance, the spectra of the wild-type bR and the D96N mutant have similar overall features; however, there are some differences. Characteristic differences can be seen above 1700 cm^{-1}.

COOH vibrations

The protonated form of carboxylic acids has a characteristic band above 1680 cm^{-1}, originating from the C=O bond stretch of the COOH group (Bellamy, 1975). In light-induced difference spectra of bR, most of the peaks were clearly assigned to single aspartic acid residues. The difference peak of the COOH vibration was found at 1761 cm^{-1} for Asp-85 (it becomes protonated in the M form), at 1742 cm^{-1} for Asp-96, ~1729–1740 cm^{-1} for Asp-115, and at 1738 cm^{-1} for Asp-212 (in the M form) (e.g., Braiman et al., 1988). Although the assignment of the band from Asp-212 is not settled (according to recent studies the band at 1738 cm^{-1} may not originate from Asp-212 (Maeda et al., 1994)), the only groups protonated in the ground state at pH = 7 are Asp-96 and Asp-115: these are the candidates to show deprotonation at higher pH.

Fig. 3, *A* and *B* show the region of COOH vibrations where pH-dependent changes were observed. The peak position

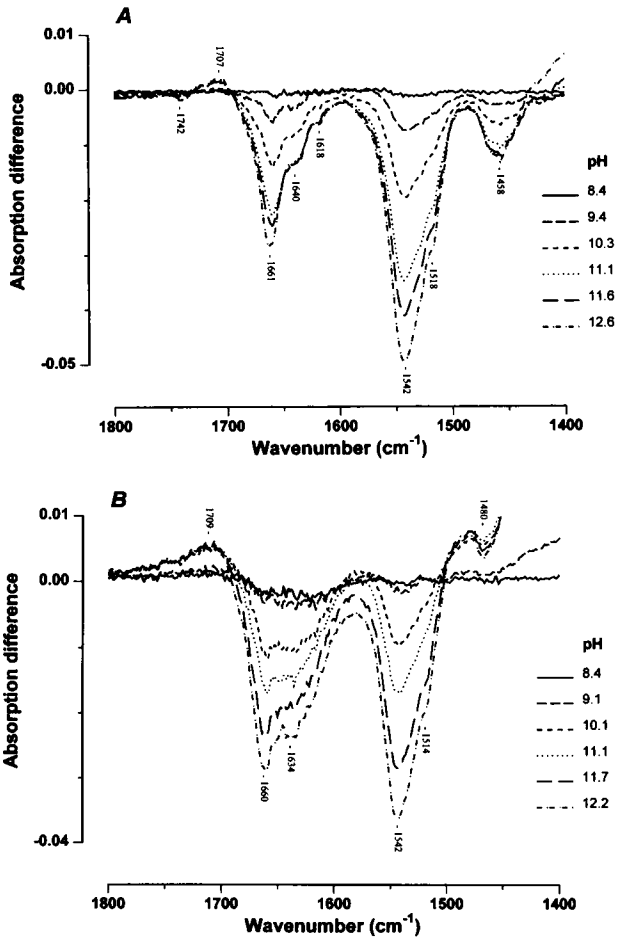

FIGURE 2 FTIR ATR difference spectra of wild-type (*A*) and D96N (*B*) bacteriorhodopsin at several pHs. (Difference spectra were calculated according to Eq. 1.)

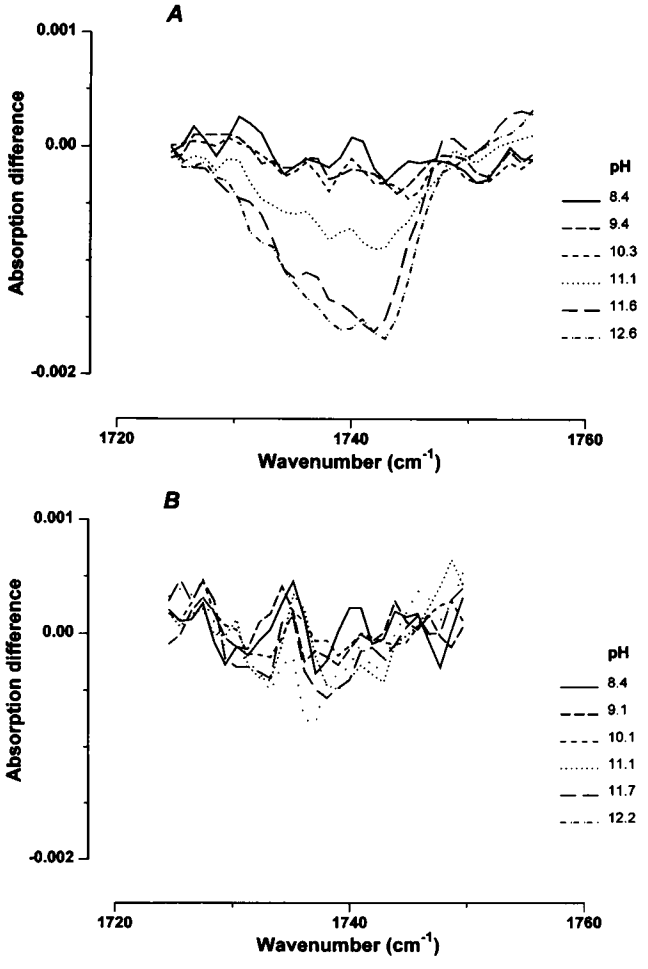

FIGURE 3 The region of the COOH vibrations where pH-induced changes were observed. (Spectra are the same as shown in Fig. 2, *A* and *B*). To get a flat baseline, a second order baseline correction was applied. (*A*, wild-type bacteriorhodopsin; *B*, D96N mutant of bacteriorhodopsin.)

(1742 cm^{-1}) and the fact that no band appears in the case of the D96N mutant make it evident that in wild-type bR Asp-96 is titrated. The band is negative because it reflects a loss of protonated Asp-96 as compared with pH = 7 upon increasing pH.

To calculate the pH dependence of the 1742 cm^{-1} peak, SVD was applied. The basis spectra multiplied by their singular values (i.e., the weighted independent basis spectra) are shown in Fig. 4, *A* and *B*. Fig. 4 *A* shows only one significant spectrum, whereas in Fig. 4 *B* no spectrum emerges from the noise. The fact that for wild-type a single significant spectrum component was found whereas none was found for the D96N mutant confirms that a single carboxylic residue undergoes protonation change, that is, Asp-96. In this case, the intensity of the 1742 cm^{-1} peak is proportional to the concentration of bR having a protonated Asp-96. The pK_a of the titration was obtained by fitting the first column of the *V* matrix by Eq. 3 as described in Materials and Methods (Fig. 5). Evaluating three sets of data, $pK_a = 11.4 \pm 0.1$ was calculated.

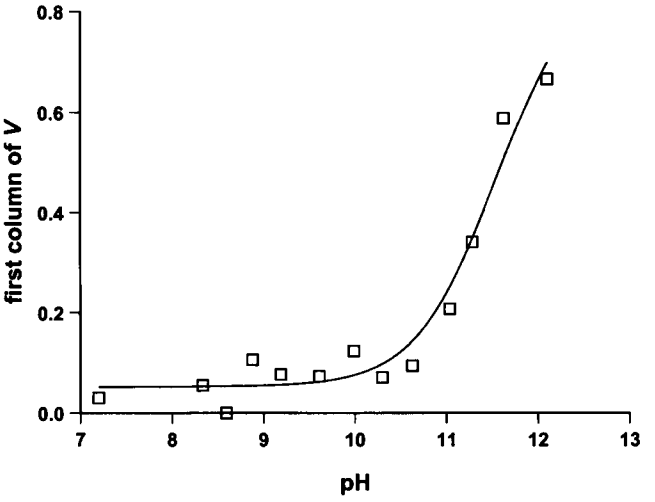

FIGURE 5 The first column of matrix *V* that describes the pH dependence of the biggest component shown in Fig. 4 (□). This curve shows the deprotonation Asp-96 (see text). The continuous line is the result of a least-square fit with the theoretical function (Eq. 3) for a single dissociating acid ($pK_a = 11.4 \pm 0.1$).

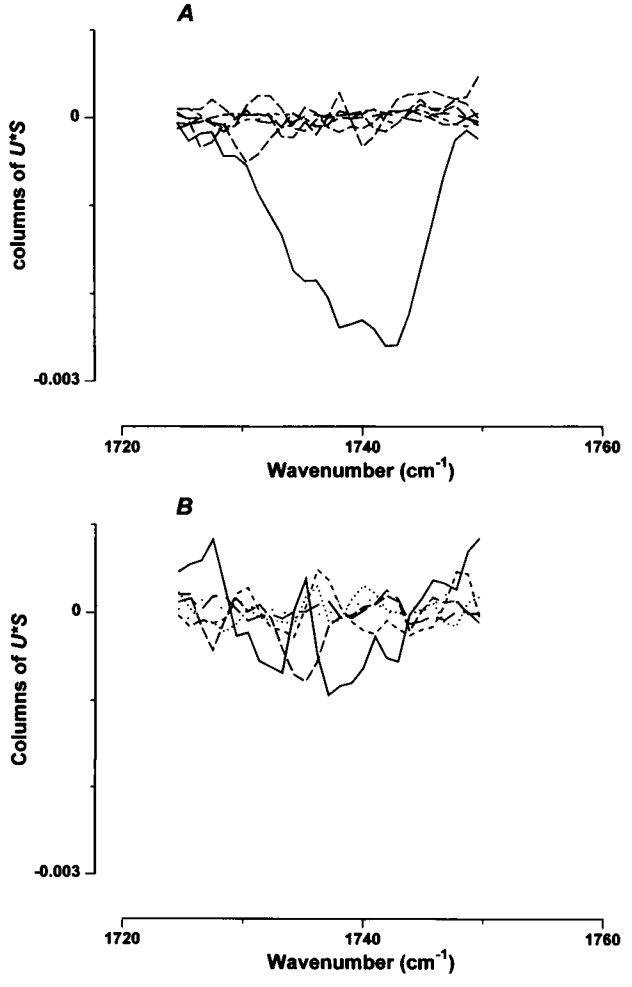

FIGURE 4 The result of singular value decomposition of the spectra shown in Fig. 3 (see Materials and Methods). Only the first six components are shown; components with higher index are negligible. (*A*, wild-type bacteriorhodopsin; *B*, D96N mutant of bacteriorhodopsin.)

pH-dependent structural changes of the protein backbone

Although the spectra in the 1450–1700 cm^{-1} region are very complex and cannot be interpreted on the basis of these experimental data, it is reasonable to assume that they are dominated by the amide-I and amide-II bands. These bands reflect changes of the protein backbone; other spectral changes caused by vibrations of single groups should be negligible compared with them. However, it is also clear that protonation or deprotonation of single amino acid residues may result in reordering of a significant part of the protein. The C=N stretching mode serves as a marker band for protonation of the retinal Schiff-base (e.g., Bagley et al., 1982). Because no exchange of a negative 1640 cm^{-1} band (protonated Schiff-base) to a positive band at 1624 cm^{-1} (deprotonated Schiff-base) can be seen in our spectra, significant deprotonation of the retinal Schiff-base can be excluded. It is in agreement with resonance Raman data where the pK_a of the chromophore was found to be ~13.3 (Druckman et al., 1982).

To get quantitative information on the conformational changes of the backbone, we applied SVD to the 1450–1700 cm^{-1} region. Similar results were obtained for the wild-type bR and the D96N mutant (Fig. 6, *A* and *B*): we found a single significant basis spectrum in both cases that was similar (peak positions are nearly the same; only their relative amplitudes differ). The higher order components of U^*S (≥ 2) are probably caused by baseline errors because they did not show meaningful pH dependence (data not shown). The first column of matrix *V* (shown in Fig. 7, *A* and *B*) that describes the pH dependence of the first basis spectrum was also similar for the wild-type and D96N bR and could be fitted assuming at least two independent titration processes ($n = 2$). The obtained numerical values are: $pK_{a1} = 9.3 \pm 0.3$, $pK_{a2} =$

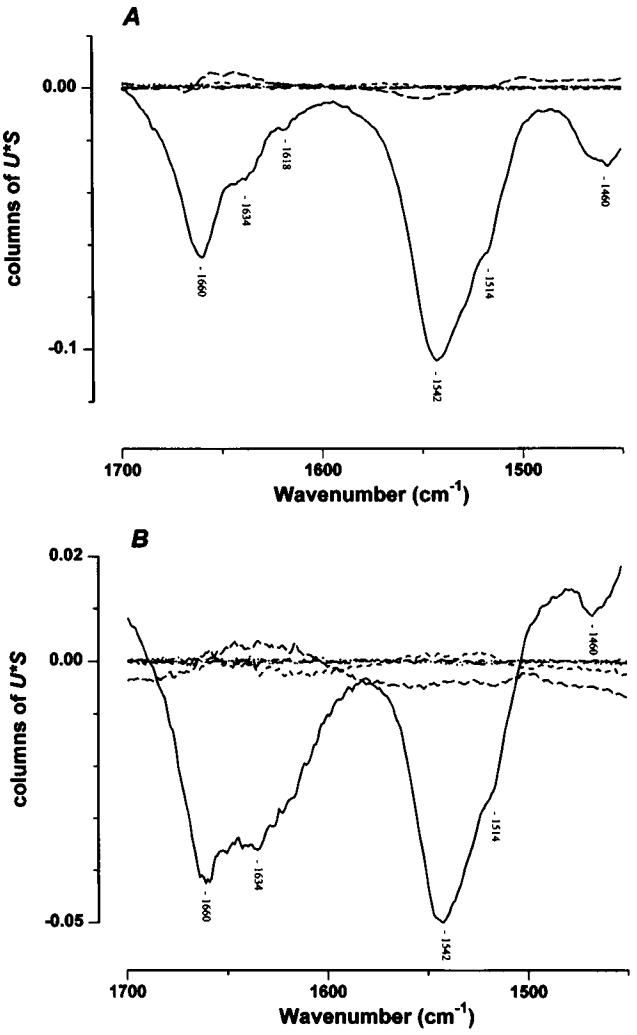

FIGURE 6 The basis spectra calculated by singular value decomposition of the spectra shown in Fig. 2 (1450–1700 cm^{-1}). This spectral range is assumed to characterize protein conformational changes. (*A*, wild-type bacteriorhodopsin; *B*, D96N mutant of bacteriorhodopsin.)

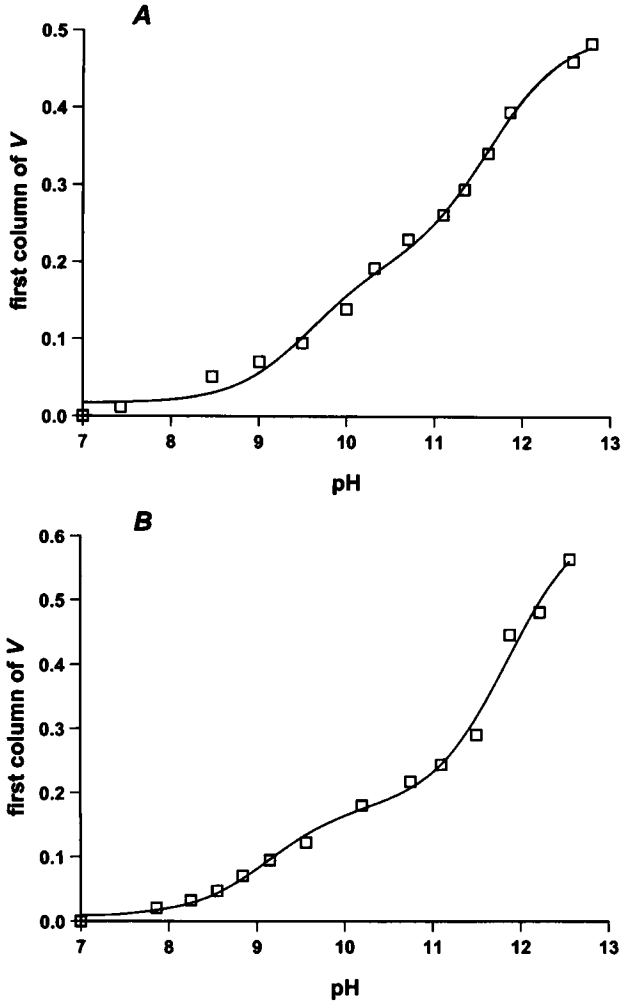

FIGURE 7 The first column of matrix *V* that describes the pH dependence of the largest component shown in Fig. 6 (□). This curve is characteristic to conformational changes of the protein backbone induced by pH change (see text). The continuous line is the result of a least-square fit with the theoretical function (Eq. 3, $n = 2$). The obtained numerical values are: $pK_{a1} = 9.3 \pm 0.3$, $pK_{a2} = 11.5 \pm 0.2$ for wild-type bR (*A*); $pK_{a1} = 9.4 \pm 0.3$, $pK_{a2} = 11.5 \pm 0.3$ for D96N (*B*), respectively.

11.5 ± 0.2 for wild-type bR; $pK_{a1} = 9.4 \pm 0.3$, $pK_{a2} = 11.5 \pm 0.3$ for D96N, respectively.

DISCUSSION

We have found that at high pH Asp-96 in dark-adapted bR becomes deprotonated with $pK_a = 11.4 \pm 0.1$ in 1 M NaCl. Because of the high salt concentration, this value should be close to the intrinsic pK_a. The absence of such a titration in the D96N mutant confirms that the 1742 cm^{-1} band is caused by Asp-96 only and that Asp-115 (which is present in the D96N mutant) should have a pK_a over 12. These results are in excellent agreement with the model calculations of Bashford and Gerwert (1992), who have found a value of 11.6 ± 1.2 for Asp-96 and 15.4 ± 8.6 for Asp-115 using constrained dynamics model calculations with the assumption that Arg-82 is pointing toward the retinal Schiff-base. On the other hand, a recently published work by Sampogna and Honig (1994) reports results with values significantly lower than our results.

The pH-dependent changes of the protein backbone could be characterized assuming at least two titrated groups with a pK_a of 9.3 ± 0.3 and 11.5 ± 0.2. Within the experimental error, the same values were found for the D96N mutant. It is a striking observation that the higher value for both the wild-type and D96N mutant is the same as that obtained for Asp-96 titration (Fig. 2 *A*). This fact suggests that deprotonation of Asp-96 is a consequence of a protein conformational change also occurring in the Asp-96-free mutant. The reasonable explanation is that the conformational change is an opening up of the protein that makes Asp-96 accessible to water. This is in accordance with Henderson et al. (1990), who describe the intracellular half of the proton channel where Asp-96 is located as narrow and highly hydrophobic. Deprotonation of Asp-96, therefore, is rather a marker of the protein conformation, in which the the accessibility of Asp-96 changes. According to our data, the titration of Asp-96 can be described with a single pK_a value; it follows,

therefore, that the transition of the protein that changes the accessibility of Asp-96 is governed by the deprotonation of a single group, naturally other than Asp-96. Concerning the protein spectra, two observations deserve special attention: 1) SVD analysis resulted in only one significant spectrum component. Consequently, in the whole pH range 7–12 a continuous conformational change takes place that is uniform in its main characteristics. 2) As far as the signal-to-noise ratio of our experiments permits, it can be concluded that all spectral changes in this pH range are determined by the protonation of only two groups.

From the present data, it is not possible to identify the specific amino acid residues responsible for the alteration of the backbone structure. Based on pH dependence of the visible and UV spectra of bR, Balashov et al. (1991) concluded that three tyrosine residues get deprotonated with a pK_a of ~9.0, 10.3, and 11.3 (in 167 mM KCl). This result agrees with our values assuming that in our case the two lower pK_a values are not distinguished. Comparison of our spectra with those in Roepe et al. (1987) where bands in the M-bR difference spectrum are reminescent of ours were assigned to tyrosine protonation also support this assumption. Further studies are being carried out to make positive identification.

This work was supported by grants from the National Scientific Research Fund of Hungary (OTKA 914 and OTKA F12917).

REFERENCES

Bagley, K., G. Dollinger, L. Eisenstein, A. K. Singh, and L. Zimányi. 1982. Fourier transform spectroscopy of bacteriorhodopsin and its photoproducts. *Proc. Natl. Acad. Sci. USA.* 79:4972–4976.

Balashov, S. P., R. Govinjee, and T. G. Ebrey. 1991. Red shift of the purple membrane absorption band and the deprotonation of tyrosine residues at high pH. *Biophys. J.* 60:475–490.

Bashford, D., and K. Gerwert. 1992. Electrostatic calculations of the pK_a values of ionizable groups in bacteriorhodopsin. *J. Mol. Biol.* 224:473–486.

Bellamy, L. J. 1975. The Infra-Red Spectra of Complex Molecules. Chapman and Hall, London.

Braiman, M. S., O. Bousché, and K. J. Rothschild. 1991. Protein dynamics in the bacteriorhodopsin photocycle: submillisecond Fourier transform infrared spectra of the L, M, and N photointermediates. *Proc. Natl. Acad. Sci. USA.* 88:2388–2392.

Braiman, M. S., T. Mogi, T. Marti, L. J. Stern, H. G. Khorana, and K. J. Rothschild. 1988. Vibrational spectroscopy of bacteriorhodopsin mutants: light-driven proton transport involves protonation changes of aspartic acid residues 85, 96, and 212. *Biochemistry.* 27:8516–8520.

Butt, H.-J., K. Fendler, E. Bamberg, J. Tittor, and D. Oesterhelt. 1989. Aspartic acids 96 and 85 play a central role in the function of bacteriorhodopsin as a proton pump. *EMBO J.* 8:1657–1663.

Dencher, N. A., J. Heberle, C. Bark, M. H. Koch, G. Rapp, D. Oesterhelt, K. Bartels, and G. Büldt. 1991. Proton translocation and conformational changes during the bacteriorhodopsin photocycle—time-resolved studies with membrane-bound optical probes and x-ray diffraction. *Photochem. Photobiol.* 54:881–887.

Dollinger, G., L. Eisenstein, S.-L. Lin S-L, K. Nakanishi, K. Odashima, and J. Termini. 1986. Bacteriorhodopsin: Fourier transform infrared methods for studies of protonation of carboxyl groups. *Methods Enzymol.* 127: 649–662.

Druckman, S., M. Ottolenghi, A. Pande, J. Pande, and R. H. Callender. 1982. Acid-base equilibrium of the Schiff-base in bacteriorhodopsin. *Biochemistry.* 21:4953–4959.

Ebrey, T. G. 1993. Light energy transduction in bacteriorhodopsin. *In* Thermodynamics of Membrane Receptors and Channels. M. B. Jackson editor. CRC Press, Boca Raton, FL. 353–387.

Fodor, S. P. A., J. B. Ames, R. Gebhard, E. M. van den Berg, W. Stoeckenius, J. Lugtenburg, and R. A. Mathies. 1988. Chromophore structure in bacteriorhodopsin's N intermediate: implications for the proton-pumping mechanism. *Biochemistry.* 27:7097–7101.

Gerwert, K. 1992. Molecular reaction mechanism of photosynthetic proteins as determined by FTIR-spectroscopy. *Biochim. Biophys. Acta.* 1101: 147–153.

Gerwert, K., B. Hess, J. Soppa, and D. Oesterhelt. 1989. Role of aspartate-96 in proton translocation by bacteriorhodopsin. *Proc. Natl. Acad. Sci. USA.* 86:4943–4947.

Gerwert, K., G. Souvignier, and B. Hess. 1990. Simultaneous monitoring of light-induced changes in protein side-group protonation, chromophore isomerisation, and backbone motion of bacteriorhodopsin by time-resolved Fourier-transform infrared spectroscopy. *Proc. Natl. Acad. Sci. USA.* 87:9774–9778.

Henderson, R., J. M. Baldwin, T. A. Ceska, F. Zemlin, E. Beckman, and K. H. Downing. 1990. Model for the structure of bacteriorhodopsin based on high-resolution electron cryo-microscopy. *J. Mol. Biol.* 213: 899–929.

Henry, E. H., and J. Hofrichter. 1992. Singular value decomposition: application to analysis of experimental data. *Methods Enzymol.* 210: 129–191.

Holz, M., L. A. Drachev, T. Mogi, H. Otto, A. D. Kaulen, M. P. Heyn, V. P. Skulachev, and H. G. Khorana. 1989. Replacement of aspartic acid-96 by asparagine in bacteriorhodopsin slows both the decay of the M intermediate and the associated proton movement. *Proc. Natl. Acad. Sci. USA.* 86:2167–2171.

Keszthelyi, L., and P. Ormos. 1989. Protein electric response signals from dielectrically polarized systems. *J. Membr. Biol.* 109:193–200.

Koch, M. H. J., N. A. Dencher, D. Oesterhelt, H.-J. Plöhn, G. Rapp, and G. Büldt. 1991. Time-resolved x-ray diffraction study of structural changes associated with the photocycle of bacteriorhodopsin. *EMBO J.* 10: 521–526.

Lanyi, J. K. 1993. Proton translocation mechanism and energetics in the light-driven proton pump bacteriorhodopsin. *Biochim. Biophys. Acta.* 1183:241–261.

Lozier, R. H., R. A. Bogomolni, and W. Stoeckenius. 1975. Bacteriorhodopsin: a light-driven proton pump in *Halobacterium halobium. Biophys. J.* 15:955–962.

Marrero, H., and K. Rothschild. 1987. Conformational changes in bacteriorhodopsin studied by infrared attenuated total reflection. *Biophys. J.* 52:629–635.

Mathies, R. A., S. W. Lin, J. B. Ames, and W. T. Pollard. 1991. From femtoseconds to biology: mechanism of bacteriorhodopsin's light-driven proton pump. *Annu. Rev. Biophys. Biophys. Chem.* 20:491–518.

Metz, G., F. Siebert, and M. Engelhard. 1992. High-resolution solid state ^{13}C NMR of bacteriorhodopsin: characterization of [4-^{13}C] resonances. *Biochemistry.* 31:455–461.

Mogi, T., L. J. Stern, T. Marti, B. H. Cao, and H. G. Khorana. 1988. Aspartic acid substitutions affect proton translocation by bacteriorhodopsin. *Proc. Natl. Acad. Sci. USA.* 85:4148–4152.

Oesterhelt, D., and W. Stoeckenius. 1974. Isolation of the cell membrane of *Halobacterium halobium* and its fractionation into red and purple membrane. *Methods Enzymol.* 31:667–678.

Oesterhelt, D., and J. Tittor. 1989. Two pumps, one principle: light driven transport in halobacteria. *Trends Biochem. Sci.* 14:57–61.

Oesterhelt, D., J. Tittor, and E. Bamberg. 1992. A unifying concept for ion translocation by retinal proteins. *J. Bioenerg. Biomembr.* 24:181–191.

Ormos, P. 1991. Infrared spectroscopic demonstration of a conformational change in bacteriorhodopsin involved in proton pumping. *Proc. Natl. Acad. Sci. USA.* 88:473–477.

Ormos, P., K. Chou, and J. Mourant. 1992. Infrared study of the L, M, N intermediates of bacteriorhodopsin using the photoreaction of M. *Biochemistry.* 31:6933–6937.

Roepe, P., P. L. Ahl, S. K. Das Gupta, J. Herzfeld, and K. J. Rothschild. 1987. Tyrosine and carboxyl protonation changes in the bacteriorhodopsin photocycle. 1. M412 and L550 intermediates. *Biochemistry.* 26:6696–6707.

Rothschild, K. J., and H. Marrero. 1982. Infrared evidence that the Schiff-base of bacteriorhodopsin is protonated: bR570 and K intermediates. *Proc. Natl. Acad. Sci. USA.* 79:4045–4049.

Sampogna, R. V., and B. Honig. 1994. Environmental effects on the protonation states of active site residues in bacteriorhodopsin. *Biophys. J.* 66:1341–1352.

Sasaki, J., J. K. Lanyi, R. Needleman, T. Yoshizawa, and A. Maeda. 1994. Complete identification of C=O stretching vibrational bands of protonated aspartic acid residues in the difference infrared spectra of M and N intermediates versus bacteriorhodopsin. *Biochemistry.* 33: 3178–3184.

Soppa, J., and D. Oesterhelt. 1989a. Bacteriorhodopsin mutants of halobacterium sp. GRB 1. The 5-bromouridine-selection as a method to isolate point mutants in halobacteria. *J. Biol. Chem.* 264: 13043–13048.

Soppa, J., J. Otomo, J. Straub, J. Tittor, S. Meessen, and D. Oesterhelt. 1989b. Bacteriorhodopsin mutants of Halobacterium spec. GRB 2. Characterization of mutants. *J. Biol. Chem.* 264:13049–13056.

Stoeckenius, W., and R. A. Bogomolni. 1982. Bacteriorhodopsin and related pigments of halobacteria. *Annu. Rev. Biochem.* 51:587–616.

Subramaniam, S., M. Gerstein, D. Oesterhelt, and R. Henderson. 1993. Electron diffraction analysis of structural changes in the photocycle of bacteriorhodopsin. *EMBO J.* 12:1–8.

Tittor, J., C. Soell, D. Oesterhelt, H.-J. Butt, and E. Bamberg. 1989. A defective pump, point-mutated bacteriorhodopsin Asp96-Asn is fully reactivated by azide. *EMBO J.* 8:3477–3482.

Turner, G. J., L. J. W. Miercke, T. E. Thorgeirsson, D. S. Kliger, M. C. Betlach, and R. M. Stroud. 1993. Bacteriorhodopsin D85N: three spectroscopic species in equilibrium. *Biochemistry.* 32:1332–1337.